CYBERNETICS AND PHYSICS, VOL. 12, NO. 4, 2023, 252–256

FEASIBILITY STUDY OF PERMANENT MAGNET DIPOLES FOR SILA FACILITY

Daria Arslanova
JSC "NIIEFA", Russia
arslanova-sci@yandex.ru

Yuri Gavrish
JSC "NIIEFA", Russia
gavrish@luts.niiefa.spb.su

Elena Gapionok
JSC "NIIEFA", Russia
gapionok-sci@yandex.ru

Aleksandra Grosheva
JSC "NIIEFA", Russia
a.d.grosheva@yandex.ru

Nikita Knyazev
JSC "NIIEFA", Russia
knyazev@sintez.niiefa.sintez.spb.su

Vladimir Kukhtin
JSC "NIIEFA", Russia
ovc74@mail.ru

Eugeny Lamzin
JSC "NIIEFA", Russia
lamzin-sci@yandex.ru

Andrey Nezhentzev
JSC "NIIEFA", Russia
nezhentzev-sci@yandex.ru

Alexander Ovsyannikov
St.Petersburg State University, Russia
ovs74@mail.ru

Dmitri Ovsyannikov, Sergey Sytchevsky,
St.Petersburg State University, Russia
dovs45@mail.ru, sytch-sie@yandex.ru

Nataliia Znamenshchikova
JSC "NIIEFA", Russia
znamenatali@gmail.com

Article history:
Received 01.12.2023, Accepted 26.12.2023

Abstract

The 40 cell lattice of the new Russian synchrotron radiation facility SILA is envisaged to employ permanent magnet (PM) dipoles as bend magnets. Numerical study of the basic concept for short PM dipoles is described. Iterative 3D simulations with a detailed model were used to assess anticipated field distribution and magnetic forces. A scope of critical aspects was investigated to move up to the engineering design including candidate materials, geometry, thermal stability, magnetic interaction, and field tuning. Aggregated results made it possible to optimize the initial concept and get guidance to practical implementation.

Key words

synchrotron source, lattice, permanent magnet, dipole, simulation

1 Introduction

One of the milestones of the Russian Federal Program for science infrastructure development is the accelerating-storage facility SILA [Ashanin et al.]. SILA is a 4th generation light source with the periodic Hybrid Multi Bend Achromat (HMBA) lattice [Raimondi, 2017] intended to operate in the range of synchrotron radiation. A high-energy storage ring of 6 GeV combined with a free electron laser enables drastic increase in brilliance of the emitted light.

The hybrid configuration offers benefits of the cost saving in operation/maintenance and ensures high gradient, compactness and tunability.

The optical and magnetic specifications for the SILA facility are loosely based on the ESRF-EBS concept [Raimondi, 2017]. High-coercivity permanent magnets are utilized as a general trend for the 4th generation sources, that provides a high field strength and absence of power supply in contrast to electromagnets. The magnet structure includes long and short PM-based dipoles which serve as bending magnets. The long PM dipoles with longitudinal gradient are placed at each end of the regular cell. An innovative design, as compared to standard multiple bend, involves the use of a short PM dipole as an additional bend magnet (SBM) located in the central part of the cell illustrated in Figure 1. Such configuration enable us to double the number of light channels.

Each SBM utilizes the Sm_2Co_{17} PM material and pure iron for the yoke and poles.

The study performed to support the long PM dipole design has revealed a noticeable effect of the material and sizes of shims intended for field tuning. Pursue of the best shim specification was one of the key issue. For

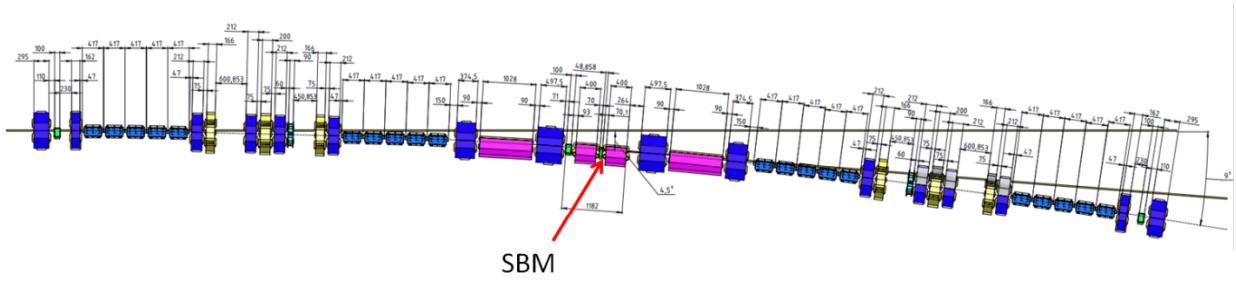

Figure 1. Layout of SILA cell with PM bend magnets.

SBM the required field quality is even harder to reach due to a shorter magnetic length.

In closed magnet systems with coils a field distribution in the magnet aperture is dictated primarily by the magnetic circuit. Field fluctuations are introduced by imperfect pole shapes, possible variations in material properties, and manufacture/assembly tolerances.

In open magnet systems with coils and/or PM the field fluctuations are associated with possible variations in parameters of conductors and PM blocks [Amoskov et al., 2021; Amoskov et al., 2022].

Configurations of electromagnets for multipole accelerators are well established [Steffen, 1965], so it is possible to adapt an existing design to a specific task. This would imply solving a direct problem of determining the field distribution with respect to specified field sources. In turn, the field tuning scheme and shim parameters are found by solving an inverse problem. Finally, the field adjustment should be made with the use of magnetic measurements at variable coil currents.

To guarantee the desired field quality in PM magnet systems different solutions need to be explored. A reach nomenclature of possible magnet configurations and PM units makes this task nontrivial. Numerical studies demonstrated that field quality is rather sensitive to possible spread of magnet parameters. A divergence of several percents in magnet specification would lead to crucial deterioration of the required field in the aperture. In fact, PM-based dipoles for SILA need a detailed specification of all PM units supplemented with results of parametric simulations and magnetic measurements. Thus, synthesis of the magnet system produces an extensive data set that needs to be processed and analyzed during design and prototyping.

To sum up, it is vital to move towards dedicated computing power and control algorithms with implementation of AI technologies [Knyazev et al., 2023] to produce, exchange and interpret a huge amount of data at all stages of R&D, commissioning and operation of the facility.

2 Short bend magnet design

The SBM design is presented schematically in Figures 2, 3. The full assembly is symmetrical that allows reduction of the computational model to one half of the magnet.

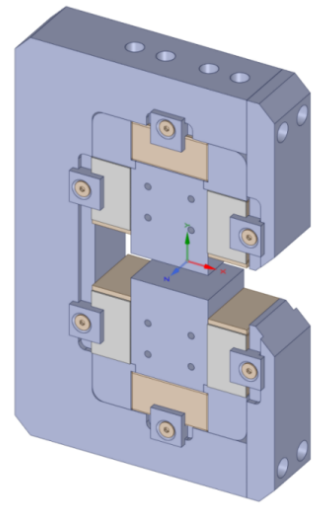

Figure 2. PM-based short bend magnet

The yoke and poles of SBM are to be made of a low-coercivity material, a suitable candidate is ARMCO. The dipole is magnetized with an assembly of PM blocks. Sm_2Co_{17} is selected due to its resistance to radiation damage and temperature stability. To prevent possible fluctuations of magnetic properties, thermal shims will be mounted at the vertical PM blocks as shown in Figure 3.

Holes 8 mm in diameter on the horizontal sides of the yoke are used to fix the PM blocks and the poles.

The resultant field is tuned with end iron shims located on the pole ends.

The sizes of the main SBM components are specified in Figure 3.

A brief material specification for SBM with respect to the desired field quality is as follows:

• Pure iron pole and yoke, with permeability $\mu \geq 7500$ and low coercivity $H_c \leq 66$ A/m);

• Sm_2Co_{17} permanent magnet material; residual induction – $B_r = 1.12$ T, coercivity $H_{cb} = 810$ kA/m;

Table 1. Integrated SBM field $\int B_y dz$ at 20°C. Structural holes are omitted

N	SBM sizes mm	h_{term}, mm	h_m, mm	$\int B_y dz$, T·m
1	168×256×40	0	1	0.041109
2	168×256×40	1	0	0.042964
3	168×256×42	1	1	0.043183
4	168×256×40	1	1	0.040960
5	168×256×40	3	1	0.040657

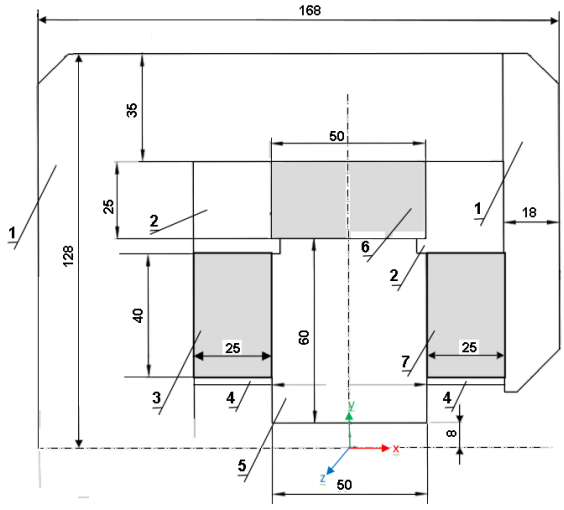

Figure 3. SBM structure over transverse cross section, 1/2 of whole assembly. 1 – iron yoke; 2 – aluminium spacer; 3,6,7 – PM blocks; 4 – FeNi thermal shims; 5 – iron pole.

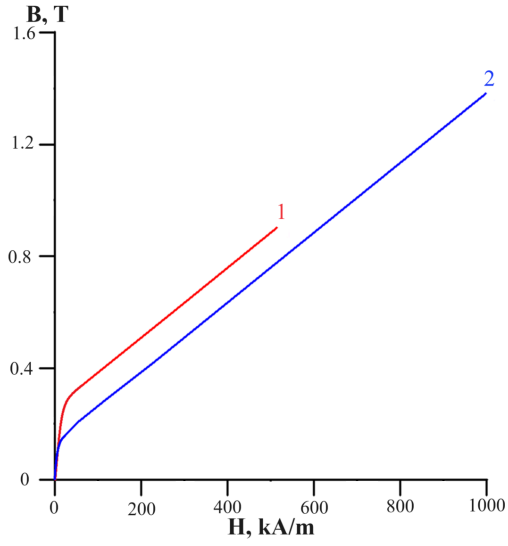

Figure 4. Temperature dependence of Fe-Ni alloy magnetic properties: 1 – at T=20°C, 2 – at T=40°C.

• Low temperature coefficient for B_r – $\alpha = -0.035\%/°C$;
• passive thermal compensation with Fe-Ni shims, the adopted $B(H)$ curves specified in Figure 4 [Pyatin, 1982].

Figure 4 demonstrates that the Fe-Ni alloy is losing its magnetic permeability with temperature rise. This leads to a fall of its shimming efficiency with consequent increase in the field in the SBM aperture.

3 Numerical optimization of SBM design

The main parameters specified for SBM design are the field in the magnet aperture of 0.8602 T and the effective length of 48.848 mm. The integrated field along the beam path is 0.04202 T·m with the allowable error of $2 \cdot 10^{-4}$ over the region of ± 13 mm.

A relevant 3D model of SBM was parametrized with respect to the following factors:
• thermal shim thickness h_{term};
• end iron shim thickness h_m;
• locations and sizes of structural holes.

The model was computed with the code KOMPOT [Amoskov et al., 2008] with ranged parameters in search of optimal performance. The simulations gave assessments for:
• field distribution at different SBM sizes as presented in Table 1 and Figure 5;
• integrated field vs thermal shim thickness and temperature, see Figures 6, 7;
• integrated field vs iron shim thickness, see Figure 8.

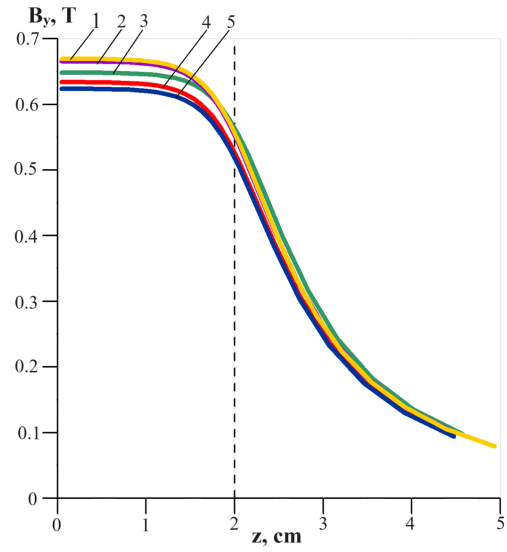

Figure 5. Vertical field along beam path for various SBM sizes. Curves are numbered according to Table 1.

Figure 5 shows simulated distributions of the vertical field along the beam path for various sizes of SBM as listed in Table 1.

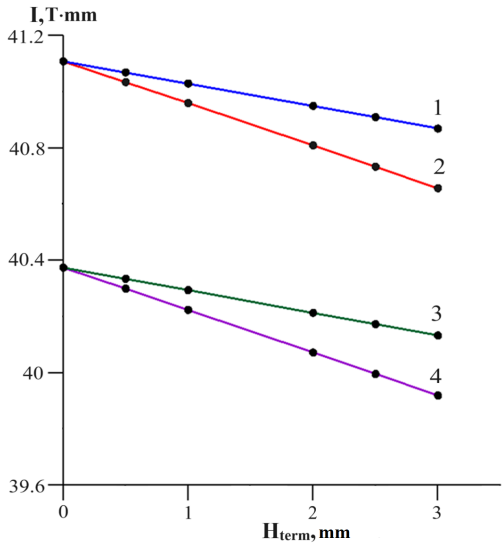

Figure 6. Integrated field vs thickness of Fe-Ni shims at various temperatures: 1 – T=40°C, no structural holes; 2 – T=20°C, no structural holes; 3 – T=40°C with structural holes; 4 – T=20°C with structural holes.

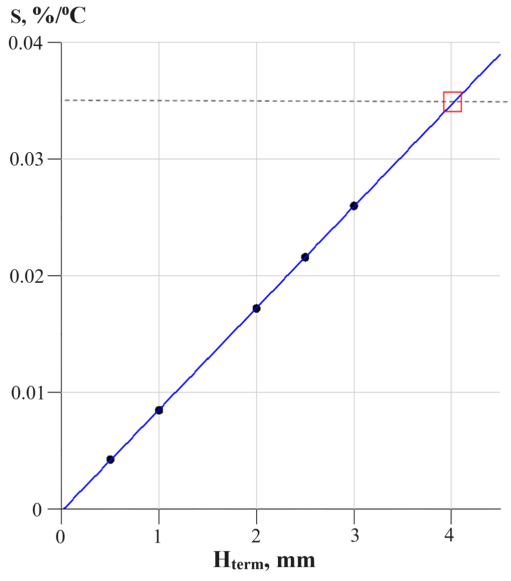

Figure 7. SBM temperature stability vs thickness of Fe-Ni shim.

Plots in Figure 6 demonstrate a linear dependence of the integrated field on the thickness of thermal shims. Design options with and without structural holes have been simulated.

Temperature fluctuations of the SBM field were estimated as:

$$S = ((I_{T2} - I_{T1})/I_{av})/\Delta T \cdot 100\%,$$

where $I = \int B_y dz$, $T1 = 20°C$, $T2 = 40°C$, $\Delta T = T2 - T1$, $I_{av} = (I_{T1} + I_{T2})/2$.

The simulation also revealed a linear dependence of the SBM thermal stability on the thickness of Fe-Ni shims. Then, to hold SBM field variations with temperature at the level $S = 0.035\%/°C$ the thickness of a Fe-Ni shim should be selected as $h_{term} = 4$ mm. This allows us to fully compensate magnetic regression of PM ($\alpha = -0.035\%/°C$). Figure 7 illustrates selection of the optimal thickness of thermal shims.

The final field tuning will be implemented with the use of iron shims. Simulated shimming efficiency is shown in Figure 8 as a function of the iron shim thickness. The plot also demonstrates a linear dependence of the integrated field on the thickness of iron shims. The proportionality constant is found to be 5.5%/mm. Therefore, the shim thickness varied within the range of 1 mm enables the field tuning to 5%.

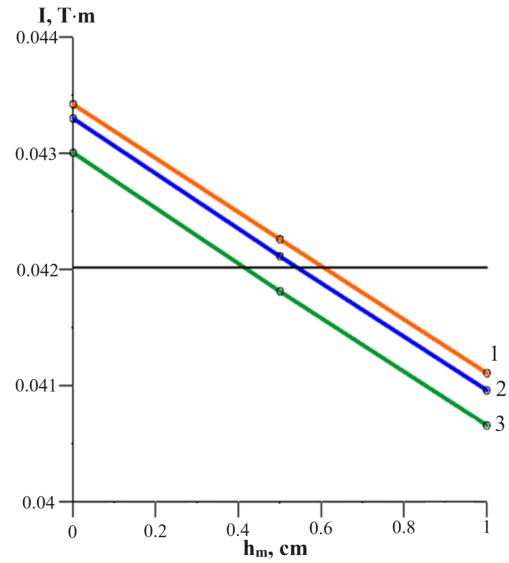

Figure 8. Integrated field at T=20°C vs iron shim thickness for various thermal shims: 1 – h_{term}=0; 2 – h_{term}=1 mm; 3 – h_{term}=3 mm.

4 Conclusions

Numerical optimization has been performed for short Sm_2Co_{17}-based dipoles of the SILA facility. The results enabled advance in the engineering design of the magnet. Parametric simulations gave solutions for a number of technological and engineering issues:

• passive thermal compensation is foreseen with the use of Fe-Ni shims. The optimal shim thickness was evaluated;

• the thickness of iron shims was selected to provide desired field tuning. It was established that 1 mm change in the thickness of an iron shim will produce field variation of 5%. Additional study should be performed to assess the field quality along the whole SBM assembly.

The optimized SBM configuration and assembly procedure will be validated on a pre-production prototype.

References

Ashanin, I.A. et al. (2018) *Physics of Atomic Nuclei*, **81**(11), pp. 1646–1651.

Raimondi, P. (2017) *Hybrid multiband achromat: From Super B to EBS*. In Proc. IPAC'17, Copenhagen, Denmark, May 14–19, pp. 3670–3675.

ESRF-EBS documentation. Available at https://www.esrf.fr/about/upgrade (Accessed: 21 November 2023)

Amoskov, V.M. et al. (2021). *VESTNIK of St.Petersburg University*, **17**(4), pp. 313–329.

Amoskov, V.M. et al. (2021). *VESTNIK of St.Petersburg University*, **18**(4), pp. 454-472.

Steffen, K.G. (1965) *High energy Beam Optics*. New York: Interscience Pub.

Knyazev N. et al. (2023). *Cybernetics and Physics*, **12**(2), pp. 129–135.

Pyatin, Yu.M. (ed.) (1982) *Materials in instrument and automatic control engineering*. Moscow: Mashinostroenie.

Amoskov, V.M. et al. (2008). *Plasma Devices and Operations*, **16**(2), pp. 89–103.